# A Novel Approach to Texture Classification using NSCT and LDBP

P. S. Hiremath
Dept. of P.G. Studies and
Research In Computer Science,
Gulbarga University, Gulbarga 585106,
Karnataka, India.

Rohini A. Bhusnurmath
Dept. of P.G. Studies and
Research In Computer Science,
Gulbarga University, Gulbarga 585106,
Karnataka, India.

## ABSTRACT
Texture is an important image feature and is defined as something consisting of mutually related elements. Texture based classification is an important approach for effective object recognition in digital images. This paper presents an efficient approach for texture classification based on local directional binary patterns (LDBP) and nonsubsampled contourlet transform (NSCT). The NSCT has translation invariability and LDBP has rotational invariability. The main focus in this study is to recognize certain directional binary patterns which are fundamental properties of local image texture. The proposed approach is robust in terms of gray scale variations, since the operator is invariant against any monotonic transformation of gray scale. The feature set is obtained by extracting statistical mean, co-occurrence parameters for three level NSCT subbands and applying LDBP for small neighborhood. Principal component analysis (PCA) is applied to avoid the curse of dimensionality. Linear discriminant analysis (LDA) ensures the class separability. The features obtained from LDA are representatives of the feature set. The evaluation of the proposed method is performed on the sixteen Brodatz textures. The k-NN classifier has been used for classification. The experimental results show a marked improvement in terms of classification accuracy.

## General Terms
Texture classification, Pattern Recognition, Image processing.

## Keywords
Texture analysis, Brodatz, Classification, LDBP, NSCT, Binary pattern

## 1. INTRODUCTION
Texture is defined as a pattern that is repeated and is represented on the surface or structure of an object. Texture remains an important and fundamental problem in computer vision and computer graphics with a wide variety of applications from synthesis, image understanding to querying by image content. A major problem in texture analysis is that textures in the real world are not uniform due to variations in orientation, scale, or other visual appearance. The gray scale invariance is important due to uneven illumination or within class variability. In addition, the degree of computational complexity of most texture analysis methods is too high. Randen and Husoy [1] concluded in their extensive comparative study of dozens of different spatial filtering methods that a very useful direction for future research is therefore the development of powerful texture measures that can be extracted and classified with low computational complexity. Most approaches to texture classification assume, either explicitly or implicitly, that the unknown samples to be classified are identical to the training samples with respect to spatial scale, orientation and gray-scale properties. But, real world textures can occur at arbitrary spatial resolutions and rotation and may be subjected to varying illumination conditions. This has inspired a development of new methods which generally incorporate invariance with respect to one or more properties, namely, spatial scale, orientation, and gray scale. A number of texture analysis tasks rely on simple statistical models such as Tamura parameters, MRF model, wavelet transform, etc. to characterize textures. The aim of the statistical model is to capture a small number of parameters so that they can be used as prior information in texture analysis fields such as texture classification, texture segmentation and texture retrieval. A simple and accurate model is an essential element in the successful texture analysis algorithm. For example, textures are classified into very smooth, smooth, medium, rough and very rough [2] based on Tamura parameters. The frequency histogram and statistical distance are used to classify textures [3]. Ojala T. [4] proposed the local binary pattern (LBP) as the texture descriptor. The few approaches on rotation invariant texture description include generalised co-occurrence matrices [5]. Invariant approach has been developed by modifying a successful non invariant approach such as Markov random field (MRF) model or Gabor filtering. The MRF based rotation invariant techniques include the circular simultaneous autoregressive model by Kashyap and khotanzad [6]. In feature based approaches, which include filtering with Gabor wavelets or other basis functions, the rotation invariance is realized by converting rotation variant features to rotation invariant features or by extracting the rotation invariant features from the filtered images [7] [8] [9] [10]. Porter and Canagrajah [11] used circular neighbour set and presented the rotation invariant generalization for wavelet, MRF, and Gabor filtering. Arof and Devari [12] obtained rotation invariant features with 1D DFT transformation, utilizing similar circular neighborhoods. Different techniques incorporating invariance with respect to both spatial scale and rotation have been presented [13] [14] [15]. Hiremath and Shivashankar [16] proposed wavelet based co-occurrence features for texture classification with k-NN classifier. Zhao et al. [17] have implemented nonsubsampled contourlet transform (NSCT), LBP to extract features and support vector machine is used as classifier. The two-phase framework of principal component analysis (PCA) and linear discriminant analysis (LDA) is found to be efficiently used in pattern recognition [18][19]. Hiremath and Rohini [20] have proposed a rotation invariant and translation invariant approach using NSCT and local direction binary patterns (LDBP) for feature extraction, and k-NN classifier for classification. In [21], authors have proposed a translation and rotation invariant texture classification using support vector machine (SVM) for classification. In the present paper, an efficient approach for texture classification using NSCT and LDBP is proposed, where the different local directional binary patterns are explored for texture description. Features are extracted using NSCT and LDBP coefficients and k-NN is

used as classifier. The proposed method is tested on Brodatz textures [22].

## 2. NONSUBSAMPLED CONTOURLET TRANSFORM

An important feature of nonsubsampled contourlet transform (NSCT) is its stability with respect to shifts of the input signals. The lack of shift invariance during image processing will cause pseudo Gibbs phenomena around singularities [23]. In order to enhance directional selectivity and shift invariance and to get rid of the frequency aliasing of contourlet, Cunha et al. [24] presented a shift invariant version of the contourlet transform namely, NSCT. To obtain a shift invariant, directional multiresolution image representation, the NSCT is built upon iterated nonsubsampled filter banks. The NSCT combines nonsubsampled pyramids to provide multi scale decomposition and nonsubsampled directional filter bank (DFB) to provide directional decomposition. The two level NSCT decomposition is shown in the Figure 1.

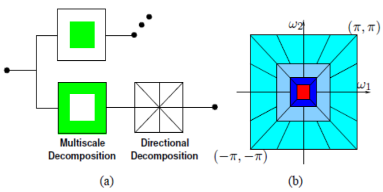


**Fig 1: Nonsubsampled contourlet transform (a) Nonsubsampled filter bank (b) Idealized frequency partitioning.**

The building block of the nonsubsampled pyramid is shown in the Figure 1(a). It is a two channel nonsubsampled filter bank which has no downsampling or upsampling and therefore is shift invariant. The ideal frequency response of a nonsubsampled DFB is shown in the Figure 1(b). The building block of a nonsubsampled DFB is a two channel nonsubsampled filter bank. The perfect reconstruction condition is given as in the Eq.(1):

$$H_0(z)G_0(z) + H_1(z)G_1(z) = 1 \tag{1}$$

A typical set of nonsubsampled contourlet coefficients of the image 'zoneplate' is shown in the Figure 2.

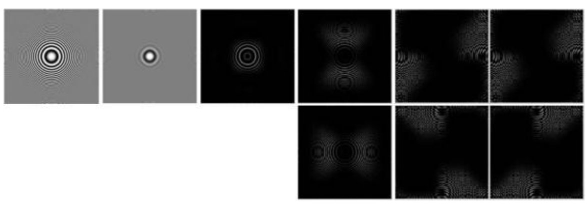

**Fig 2: Examples of the nonsubsampled contourlet transform on the zoneplate image**

## 3. LOCAL DIRECTIONAL BINARY PATTERNS

In a gray scale texture image, let the texture T in a local neighborhood of a pixel be considered as the joint distribution of the gray level of the p neighbouring pixels, and it is given by the Eq.(2):

$$T = t(f_c, f_0, \ldots, f_{p-1}), \tag{2}$$

where gray value $f_c$ corresponds to the gray value of the center pixel of the local neighborhood and $f_0, f_1, \cdots, f_{p-1}$ correspond to the gray values of p pixels with radial distance d (d>0) from the central pixel. The different local directional binary patterns (LDBPs), that are explored, are given in the Table 1.

**Table 1. Different local directional binary patterns (LDBPs) representing neighborhood (nh) with radial distance (d)**

| LDBPs | neighborhood (nh) with distance (d) |
|---|---|
| LDBP1 | 8 nh with d=1 |
| LDBP2 | {8 nh with d=1} ∪ {4 nh with d=2} |
| LDBP3 | {16 nh with d=2} ∪ {8 nh with d=1} |
| LDBP4 | 16 nh with d=2 |
| LDBP5 | 24 nh with d=3 |
| LDBP6 | {24 nh with d=3} ∪ {16 nh with d=2} |
| LDBP7 | {24 nh with d=3} ∪ {8 nh with d=1} |
| LDBP8 | {24 nh with d=3} ∪ {16 nh with d=2} ∪ {8 nh with d=1} |

The local directional binary patterns given in the Table 1 are diagrammatically shown in the Figure 3. To achieve gray scale invariance, the gray value of center pixel $f_c$ is subtracted from the gray values of the pixels in the neighborhood $f_p$, as given in the Eq.(3):

$$T = t\left(f_c, f_0 - f_c, f_1 - f_c, \cdots\cdots, f_{p-1} - f_c\right) \tag{3}$$

We assume that differences $f_p - f_c$ are independent of $f_c$, which allows to factorize Eq.(3) as in the Eq.(4):

$$T = t(f_c)\ \ t\left(f_0 - f_c, f_1 - f_c, \cdots\cdots, f_{p-1} - f_c\right) \tag{4}$$

In practice, an exact independence is not warranted. Therefore the factorized distribution is only an approximation of the joint distribution. The possible small loss in information is acceptable as it ensures invariance with respect to shifts in gray scale. In the Eq.(4), the distribution $t(f_c)$ describes the overall luminance of the image, which is unrelated to local image texture and does not provide useful information for texture analysis. Most of the information about the textural characteristics is extracted by the joint difference distribution [26] given by the Eq.(5):

$$T \approx t\left(f_0 - f_c, f_1 - f_c, \cdots\cdots, f_{p-1} - f_c\right) \tag{5}$$

This texture operator is highly discriminative. For constant regions, the differences are zero in all directions. The operator records zero values along the edge and high difference value across the edge.

Signed differences $f_p - f_c$ are not affected by changes in mean luminance. Hence, the joint difference distribution is invariant against gray-scale shifts. The scaling invariance of the gray scale is achieved by considering just the signs of the differences instead of exact values as given in the Eq.(6):

$$T \approx t\left(v(f_0 - f_c), v(f_1 - f_c), \cdots\cdots, v(f_{p-1} - f_c)\right) \tag{6}$$

where

$$v(x) = \begin{cases} 1 & x \geq 0, \\ 0 & x < 0. \end{cases} \tag{7}$$

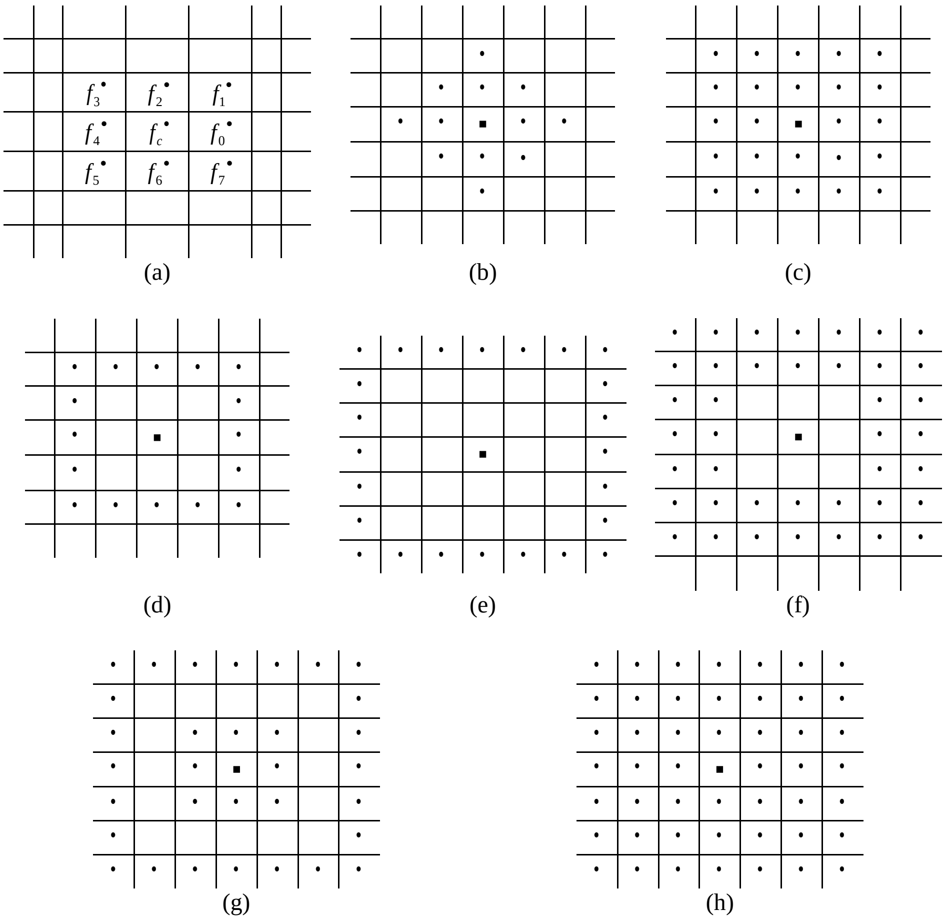

Fig 3: Local directional binary patterns (a) LDBP1, (b) LDBP2, (c) LDBP3, (d) LDBP4, (e) LDBP5, (f) LDBP6, (g) LDBP7, (h) LDBP8, of the Table 1.

By assigning a cosine factor $\cos(\theta * 360/p)$ for each sign $v(f_p - f_c)$, the Eq.(6) is transformed into unique LDBP number by converting a signal from a spatial representation into frequency representation.

$$LDBP = \sum_{p=0}^{p-1} v(f_p - f_c)\cos(p * z) \qquad (8)$$

where

$$z = 360/p$$

An image in this transform is represented as sum of sinusoids of changing magnitude and frequencies. In LDBP, a local neighborhood is thresholded at the gray value of the centre pixel into a binary pattern. The LDBP operator is invariant against any monotonic transformation of the gray scale, i.e. if the gray values in the image stays same, the output of LDBP operator remains constant.

## 3.1 Multiresolution Analysis

We have presented a gray scale invariant operator for characterising the spatial pattern using a neighborhood (nh) set of p pixels placed at radial distance of d. By altering nh and d we can implement operator for any quantization of the angular space. Multiresolution analysis can be achieved by combining the information provided by multiple operators of varying (nh,d) as listed in the Table 1. In this paper, we perform straight forward multiresolution analysis by defining the combination of dissimilarity to form the training set by extracting the responses of transform used in the section 2 and the operator in the Eq.(8).

# 4. THE PROPOSED METHOD FOR TEXTURE IMAGE CLASSIFICATION

The block diagram of the proposed method is shown in the Figure 4. The proposed method is experimented on sixteen texture images taken from Brodatz album [22]. Each image represents one texture class. Texture images of the size 256x256, are considered for the experimentation.

## 4.1 Texture Feature Extraction

Feature extraction is an essential step for pattern recognition and machine learning problems. For feature extraction, Harlick features and statistical mean (μ) are considered in the proposed method. Each texture image is divided into equal sized nonoverlapping blocks of size 64x64. The 50% of the randomly chosen blocks are considered for training and remaining blocks for testing in case of each texture class. Each block of the texture image is decomposed upto third level by nonsubsampled contourlet transform. Thus fifteen subbands for level three of NSCT decomposition are obtained. The statistical mean (μ) and Harlick features, namely, contrast, energy, entropy, homogeneity, maximum probability, cluster shade and cluster prominence are obtained for each NSCT subband coefficients to construct feature vector T1. The LDBP weights of each block are calculated to form the feature set T2, containing 3844 features for LDBP1 (=62*62 as image edges are excluded).

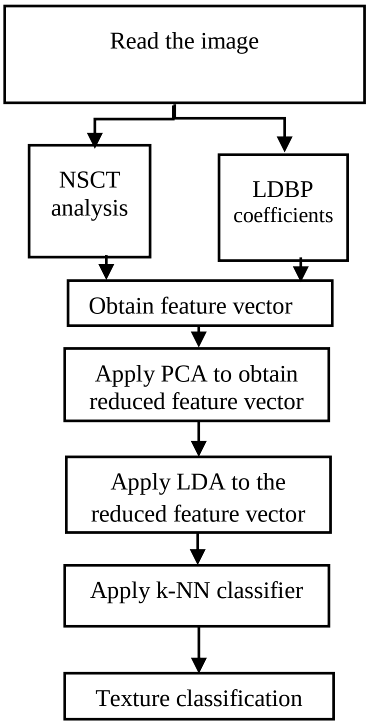


**Fig 4: Block diagram of the proposed method**

The steps of the proposed texture feature extraction are given in the Algorithm 1.

**Algorithm 1: Feature extraction algorithm**

Step 1: Input the training image block I of size 64x64
Step 2: Apply NSCT method to the image I in the Step 1.
Step 3: Compute Harlick features and mean (8 features) from each of the NSCT subbands (15 subbands) to construct feature vector T1 with 120 (=8*15) features.
Step 4: Compute LDBP1 weights for different neighborhoods (nh) with radial distance d for the image I to construct feature vector T2, which consists of 3844 features (=62*62, since the image edges are excluded).
Step 5: Form the feature vector T=(T1,T2), which contains 3964 (=120+3844) features and store T in the feature database.
Step 6: Repeat the Steps 1-5 for all the training blocks of all the texture class images and obtain the training set (TF) of feature vectors of all the texture classes.
Step 7: Apply PCA on training feature set (TF) of Step 6 to obtain reduced feature set (TFPCA).
Step 8: Apply LDA on reduced feature set (TFPCA) of Step 7 to obtain the discriminant feature set (TFLDA). Store TFLDA in the feature library, which is to be used for texture classification. Denote feature vector in TFLDA as $T_{(lib)}$ vector.
Step 9: Stop

The training Algorithm 1 is experimented using different LDBPs, which are described in the Table 1, in the Step 4. Further, the training Algorithm 1 is also implemented using Harlick features (7 features) only, for all the subbands of NSCT in the Step 3, for the purpose of comparative analysis.

## 4.2 Texture Classification

The k-NN classifier [25] is used for texture classification. If $T_{(test)}(x)$ is the feature vector of test sample image $x$ and $T_{(lib)}(m)$ is the feature vector of the m$^{th}$ class in the feature library, then the Euclidean distance between these two vectors is given by the Eq.(9):

$$D(T_{test}, T_{lib}) = \sqrt{\sum_{i=1}^{N} \left(T_{(test)i}(x) - T_{(lib)i}(m)\right)^2} \qquad (9)$$

where N is the number of features in the feature vector. The experiments are carried out using k-NN classifier with k=3. The testing algorithm is given the Algorithm 2.

**Algorithm 2: Testing algorithm (Classification of test images)**

Step 1: Input the testing image block $I_{test}$ of size 64x64
Step 2: Apply NSCT method to the image $I_{test}$.
Step 3: Compute Harlick features and mean (8 features) from each of the NSCT subbands (15 subbands) to construct feature vector $T1_{test}$ with 120 (=8*15) features.
Step 4: Compute LDBP1 weights for different neighborhoods (nh) with radial distance d for the image $I_{test}$ to construct feature vector $T2_{test}$, which consists of 3844 features (=62*62, since the image edges are excluded).
Step 5: Form the feature vector $T_{test}$ =($T1_{test}$, $T2_{test}$), which contains 3964 (=120+3844) features and store $T_{test}$ in the feature database.
Step 6: Project $T_{test}$ on TFPCA components and obtain the weights $T_{testPCA}$, which are considered as test image features.
Step 7: Project $T_{testPCA}$ on TFLDA components and obtain the weights $T_{testLDA}$, which are considered for classification. Denote $T_{testLDA}$ as $T_{(test)}$.
Step 8: (Classification) Apply k-NN classifier (k=3) to classify the test image $I_{test}$ as belonging to class m, where m=1, 2,..., 16, using Euclidean distance defined by the Eq.(9).
Step 9: Stop

The testing Algorithm 2 is experimented for different LDBPs listed in the Table 1. Further, the testing Algorithm 2 is also implemented using Harlick features (7 features) only, for all the subbands of NSCT in the Step 3.

# 5. EXPERIMENTAL RESULTS AND DISCUSSION

## 5.1 Image Dataset

The experiments are conducted by using the texture images taken from Brodatz texture album [22]. Each texture image represents a texture class, and it is of 256x256 pixels with 256 gray levels (Figure 5). Each texture image is divided into 16 nonoverlapping blocks of size 64x64 pixels. Thus 256 blocks are obtained. In order to estimate the performance of texture classification, the training and testing sets should be independent and randomly divided. The 50% of the blocks of each texture image are used as training set and remaining 50% of blocks are used as testing set.

## 5.2 Experimental Results

The experimentation of the proposed method is carried out on Intel® Core™ i3-2330M @ 2.20 GHz with 4GB RAM using MATLAB 7.9. In the proposed approach, the NSCT is performed to extract the features due to the notable properties of NSCT, namely, (i) The capability of NSCT to capture the directional edges of image at different scale, (ii) Efficiency of

NSCT in representing smooth contours in different directions of an image, (iii) Better representation of sparsity of images, and (iv) Efficient handling of 2D singularities, i.e. edges.

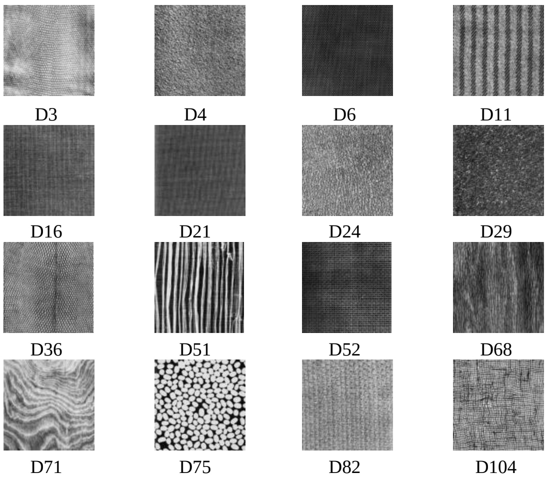


**Fig 5: Texture images from Brodatz album**

The image is decomposed using NSCT at three different resolution levels, which forms fifteen subbands. For each resolution level, it is decomposed into $2^n$ subbands, where n=0,1,2,......, which is the order of the directional filter. Since the transform is nonsubsampled, each subband corresponds to actual size of input texture image. Further, the features for each level are derived from gray level co-occurrence matrix (GLCM) with unit distance. The features are, statistical mean and Harlick texture features, namely, energy, entropy, homogeneity, maximum probability, cluster shade and cluster prominence.

The local direction binary patterns (LDBP) approach is used to detect 'uniform' local directional binary patterns at circular neighborhoods of any quantization of the angular space and at any spatial resolution. We derive the operator for a general case based on neighborhood set (nh) with radial distance d, denoting the operator as LDBP. Parameter nh controls the quantization of the angular space and d determines the spatial resolution of the operator. In addition to evaluating the performance of individual operators of particular nh and d, we propose an approach for multiresolution analysis, which combines the responses of multiple operators experimented with different nh and d. The local directional binary patterns detect microstructure (e.g. edges, lines, spots, flat areas). Spatial pattern is affected by rotation, contrast is not. Contrast is affected by the gray scale, spatial pattern is not. Consequently, for pure gray-scale invariant texture analysis, contrast is of no interest as it depends on the gray scale. So only mean is considered in the experimentation. The advantage is computational simplicity as the operator can be realized with a few operations in a small neighborhood.

The feature set so obtained with NSCT and LDBP1 has the dimension of 3964, which is very high, for the proposed method, and it has 3949 features in case of proposed method with Harlick features alone. To reduce the dimensionality of the feature set and the redundant information (i.e. the information contained in some highly correlated features) and to improve class separability, the combination of the two statistical analysis techniques PCA-LDA is used. The k-NN classifier is applied for texture image classification.

The implementation of the NSCT is based on the orientation filtering and pyramid filtering. Experiments are carried out using different Laplacian pyramidal (LP) filters for each of the different directional filters (DFB). Four categories of pyramidal filters, namely, 'pyr', '9-7', 'maxflat' and 'pyrexc' are considered, while fifteen categories of directional filters, namely, 'haar', 'dmaxflat4', ' dmaxflat5', 'dmaxflat6', 'dmaxflat7', 'qmf2', 'qmf', 'lax', 'pkva', 'ko', 'sinc', 'sk', 'vk', 'cd', 'dvmlp' filters are considered. All pairs of pyramidal filter and directional filter of NSCT for level 3 have been investigated for different LDBPs. The results of the extensive experimentation are summarised in the Table 2. The proposed method for LDBP1 with Harlick features implemented in [20] shows optimal average classification accuracy of 98.4375% with optimal pair of filters for directional filter 'dmaxflat6' and pyramidal filter 'pyrexc'. It can be concluded from the Table 2 that the proposed method offers good classification performance considering Harlick features and mean (μ). It is observed that LDBP2 gives better classification accuracy for the combination of directional filter 'haar' and pyramidal filter 'pyr' of NSCT.

**Table 2. The average classification accuracy (%) of the proposed method using optimal pair of filters of NSCT for LDBP$_S$**

| LDBP | Proposed method with Harlick features only | | Proposed method with Harlick features and mean (μ) | |
|---|---|---|---|---|
| | **Optimal Pair of Filters of NSCT** | **Average Classification Accuracy (%)** | **Optimal Pair of Filters of NSCT** | **Average Classification Accuracy (%)** |
| LDBP1 | (i)dmaxflat6, pyrexc | 98.4375 [20] | (i)dmaxflat6, pyrexc | 99.2187 |
| LDBP2 | (i) haar, pyr<br>(ii)haar, pyrexc<br>(iii)dmaxflat7, pyr<br>(iv)dmaxflat7, maxflat<br>(v) qmf2, pyrexc<br>(vi) lax, pyr | 98.4375 | (i) haar, pyr | **100** |
| LDBP3 | (i)dmaxflat5, pyrexc<br>(ii)dmaxflat6, pyrexc<br>(iii) qmf2, pyrexc | 98.4375 | (i) haar, pyr | 99.2187 |
| LDBP4 | (i) dmaxflat5, 9-7 | 96.0937 | (i)dmaxflat7, maxflat | 97.6563 |
| LDBP5 | (i) haar, pyrexc | 96.8750 | (i) dmaxflat4, pyr | 97.6563 |
| LDBP6 | (i)dmaxflat4, pyr | 96.8750 | (i) haar, pyr | 98.4575 |
| LDBP7 | (i) dmaxflat4, pyr | 96.8750 | (i) dmaxflat4, pyr<br>(ii)dmaxflat4, maxflat<br>(iii)dmaxflat5, pyr | 97.6562 |
| LDBP8 | (i) lax, pyr | 97.6563 | (i) haar, pyrexc<br>(ii) dmaxflat4, 9-7 | 98.4375 |

The Table 3 shows average classification accuracy (%) of the proposed method for LDBP2 using different directional filters and pyramidal filters of NSCT (level 3) for 16 texture categories of Brodatz [22] . It is observed from Table 3 that the proposed method with directional filter 'haar' and pyramidal filter 'pyr' has yielded optimal average classification accuracy of 100% with fifteen directional subbands and LDBP2.

The Table 4 shows the comparison of classification accuracies for texture classes obtained by the proposed method using 'haar' and 'pyr' as optimal pair of 2-D directional filter, pyramidal filter for LDBP2 and the method in [20] which is implemented on LDBP1 for 'dmaxflat6' and 'pyrexc' as optimal pair of 2-D directional filter, pyramidal filter. The experimental results demonstrate that the proposed method outperforms other texture classification methods in the literature.

**Table 3. Average classification accuracy (%) of the proposed method for LDBP2 using different directional filters and pyramidal filters of NSCT (level 3) for 16 texture categories of Brodatz [22].**

| Sl. No. | Directional Filters for NSCT | Average Classification Accuracy (%) | | | |
|---|---|---|---|---|---|
| | | Pyramidal Filters of NSCT | | | |
| | | pyr | maxflat | 9-7 | pyrexc |
| 1 | haar | **100** | 94.5313 | 93.7500 | 96.0938 |
| 2 | dmaxflat4 | 97.6563 | 98.4375 | 93.7500 | 96.0938 |
| 3 | dmaxflat5 | 95.3125 | 98.4375 | 96.8750 | 98.4375 |
| 4 | dmaxflat6 | 98.4375 | 95.3125 | 96.0938 | 96.8750 |
| 5 | dmaxflat7 | 97.6563 | 96.8750 | 96.0938 | 97.6563 |
| 6 | qmf2 | 97.6563 | 95.3125 | 95.3125 | 96.8750 |
| 7 | qmf | 96.8750 | 95.3125 | 93.7500 | 94.5313 |
| 8 | lax | 98.4375 | 98.4375 | 92.1875 | 95.3125 |
| 9 | pkva | 94.5313 | 94.5313 | 92.1875 | 97.6563 |
| 10 | ko | 96.0938 | 96.0938 | 95.3125 | 96.0938 |
| 11 | sinc | 95.3125 | 92.9688 | 95.3125 | 93.7500 |
| 12 | sk | 97.6563 | 94.5313 | 96.8750 | 95.3125 |
| 13 | vk | 97.6563 | 95.3125 | 94.5313 | 96.8750 |
| 14 | cd | 92.9688 | 96.0938 | 95.3125 | 91.4063 |
| 15 | dvmlp | 98.4375 | 89.0625 | 92.9688 | 95.3125 |

**Table 4. Comparison of classification accuracies (%) by proposed method and the method in [20] for 16 texture categories**

| Sl. No. | Image Name (Brodatz) | Hiremath and Rohini [20] (15 features) | Proposed method (15 features) |
|---|---|---|---|
| 1 | D104 | 100 | 100 |
| 2 | D11 | 100 | 100 |
| 3 | D16 | 100 | 100 |
| 4 | D21 | 100 | 100 |
| 5 | D24 | 100 | 100 |
| 6 | D29 | 100 | 100 |
| 7 | D3 | 100 | 100 |
| 8 | D36 | 87.5 | 100 |
| 9 | D4 | 100 | 100 |
| 10 | D51 | 100 | 100 |
| 11 | D52 | 100 | 100 |
| 12 | D6 | 100 | 100 |
| 13 | D68 | 100 | 100 |
| 14 | D71 | 100 | 100 |
| 15 | D75 | 100 | 100 |
| 16 | D82 | 87.5 | 100 |
| Mean classification rate | | 98.4375 | 100.0 |

# 6. CONCLUSION

In this paper, a novel texture classification method is proposed. The NSCT has translation invariability and the LDBP has rotational invariability. The LDBP operates on a local image texture to recognize certain directional binary patterns. The different local directional binary patterns are explored. The high dimensionality of feature set so obtained from NSCT and LDBP is reduced using principal component analysis (PCA) and class separability is enhanced using linear discriminant analysis (LDA). The experimentation is performed on texture images from Brodatz database. The classification is performed using k-NN classifier with k=3. The experimental results suggest that complementary information of local spatial patterns and mean plays an important role in texture discrimination. The proposed method yields better results in terms of classification accuracy in comparison with other methods in the literature.

# 7. ACKNOWLEDGMENTS

The authors are indebted to the reviewers for their detailed review, valuable comments and constructive suggestions.

# 8. REFERENCES

[1] Randen, T. and Husoy, J. H. 1999. "Filtering for Texture Classification: A Comparative Study", IEEE Trans. Pattern Analysis and Machine Intelligence", vol. 21, pp. 291-310.

[2] Lin, H. C., Chiu, C. Y., and Yang, S. N. 2002. "Texture Analysis and Description in Linguistic Term", In: The 5th Asian Conference on Computer Vision, pp. 205-209.

[3] Liu, X., Wang, D. L. 2003. "Texture Classification Using Spectral Histograms", IEEE Transactions on Image Processing, vol. 12, no. 6, pp. 661-670.

[4] Ojala, T., Pietikainen, M., and Harwood, D. 1996. "A Comparative Study of Texture Means with Classification Based on Feature Distributions", Pattern Recognition, vol. 29, no. 1, pp. 51–59.

[5] Davis, L. S., Johns, S. A., and Aggarwal, J. K. 1979. "Texture Analysis Using Generalized Cooccurrence Matrices", IEEE Trans. Pattern Analysis and Machine Intelligence, vol. 1, pp. 251- 259.

[6] Kashyap, R. L. and Khotanzad, A. 1986. "A Model-Based Method for Rotation Invariant Texture Classification", IEEE Trans. Pattern Analysis and Machine Intelligence, vol. 8, pp. 472- 481.

[7] Fountain, S. R. and Tan, T. N. 1998. "Efficient Rotation Invariant Texture Features for Content-Based Image Retrieval", Pattern Recognition, vol. 31, pp. 1725-1732.

[8] Haley, G. M. and Manjunath, B. S. 1999. "Rotation-Invariant Texture Classification Using a Complete Space-Frequency Model", IEEE Trans. Image Processing, vol. 8, pp. 255-269.

[9] Porat, M. and Zeevi, Y. 1989. "Localized Texture Processing in Vision: Analysis and Synthesis in the Gaborian Space", IEEE Trans. Biomedical Eng., vol. 36, pp. 115-129.

[10] You, J. and Cohen, H. A. 1993. "Classification and Segmentation of Rotated and Scaled Textured Images Using Texture 'Tuned' Masks", Pattern Recognition, vol. 26, pp. 245-258.

[11] Porter, R. and Canagarajah, N. 1997. "Robust Rotation-Invariant Texture Classification: Wavelet, Gabor Filter and GMRF Based Schemes", IEE Proc. Vision, Image, and Signal Processing, vol. 144, pp. 180-188.

[12] Arof, H. and Deravi, F. 1998. "Circular Neighborhood and 1-D DFT Features for Texture Classification and Segmentation", IEE Proc. Vision, Image, and Signal Processing, vol. 145, pp. 167-172.

[13] Leung, M. M. and Peterson, A. M. 1992. "Scale and Rotation Invariant Texture Classification", Proc. 26th Asilomar Conf. Signals, Systems, and Computers, vol. 1, pp. 461-465.

[14] Manian, V. and Vasquez, R. 1998. "Scaled and Rotated Texture Classification Using a Class of Basis Functions", Pattern Recognition, vol. 31, pp. 1937-1948.

[15] Wu, Y. and Yoshida, Y. 1995. "An Efficient Method for Rotation and Scaling Invariant Texture Classification", Proc. IEEE Int'l Conf. Acoustics, Speech, and Signal Processing, vol. 4, pp. 2519-2522.

[16] Hiremath, P. S. and Shivashankar, S. 2006. "Texture Classification Using Wavelet Packet Decomposition", ICGST Int. Journal on Graphics, Vision and Image Processing, vol. 6, no. 2 (Sept. 2006), pp. 77-80.

[17] Zhu, Zhengli., Zhao, Chunxia., and Hou, Yingkun. 2010. "Texture Image Classification Based on Nonsubsampled Contourlet Transform and Local Binary Patterns", Int. Journal of Digital Content Technology and Its Applications, vol. 4, no. 9, pp. 186-193.

[18] Ghafoor, Arif. 1995. "Multimedia Database Management System", ACM Comput. Surv., vol. 27, no. 4, pp. 593-598.

[19] Shivashankar, S. and Hiremath, P. S. 2011. "PCA plus LDA on Wavelet Co-Occurrence Histogram Features for Texture Classification", Int. Journal of Machine Intelligence, vol. 3, no. 4, pp. 302-306.

[20] Hiremath, P. S. and Bhusnurmath, Rohini. A. 2013. "Texture Image Classification Using Nonsubsampled Contourlet Transform and Local Directional Binary Patterns", Int. Journal of Applied Research in Computer Science and Software Engineering, vol. 3, no. 7 (July 2013), pp. 819-827.

[21] Hiremath, P. S. and Bhusnurmath, Rohini. A. 2013. "Nonsubsampled Contourlet Transform and Local Directional Binary Patterns for Texture Image Classification Using Support Vector Machine", International Journal of Engineering Research & Technology, vol. 2, no. 10 (October 2013), pp. 3881-3890.

[22] Brodatz, P. 1966. "Textures: A Photographic Album of Artists and Designers," Dover publication, New York.

[23] Coifman, R. R. and Donoho, D. L. 1995. "Translation Invariant Denoising in Wavelets and Statistics". Lecture Notes in Statistics, pp. 125-150.

[24] Cunha, A. L., Zhou, J., and Do, M. N. 2006. "The Nonsubsampled Contourlet Transform: Theory, Design and Applications". IEEE Trans. Image Processing, vol. 15, no.10, pp. 3089-3101.

[25] Duda, R. O., Hart, P. E. and Stork. 2001. Pattern Classification, Wiley publication, New York.

[26] Ojala, T., Valkealahti, K., Ojala, E., and PietikaÈinen, M. 2001. "Texture Discrimination with Multi-Dimensional Distributions of Signed Gray Level Differences", Pattern Recognition, vol. 34, pp. 727- 739.